Letter | Editors' Suggestion

Theory for tunnel magnetoresistance oscillation

Keisuke Masuda,[1,*] Thomas Scheike,[1] Hiroaki Sukegawa,[1] Yusuke Kozuka,[2] Seiji Mitani,[1,3] and Yoshio Miura[1,4,5]

[1]*Research Center for Magnetic and Spintronic Materials, National Institute for Materials Science (NIMS), Tsukuba 305-0047, Japan*
[2]*Research Center for Materials Nanoarchitectonics, National Institute for Materials Science (NIMS), Tsukuba 305-0047, Japan*
[3]*Graduate School of Science and Technology, University of Tsukuba, Tsukuba 305-8577, Japan*
[4]*Faculty of Electrical Engineering and Electronics, Kyoto Institute of Technology, Matsugasaki, Sakyo-ku, Kyoto 606-8585, Japan*
[5]*Center for Spintronics Research Network, Graduate School of Engineering Science, Osaka University, Toyonaka, Osaka 560-8531, Japan*

(Received 17 June 2024; revised 25 March 2025; accepted 23 May 2025; published 9 June 2025)

The universal oscillation of the tunnel magnetoresistance (TMR) ratio as a function of the insulating barrier thickness in crystalline magnetic tunnel junctions (MTJs) is a long-standing unsolved problem in condensed matter physics. To explain this, we here introduce a superposition of wave functions with opposite spins and different Fermi momenta, based on the fact that spin-flip scattering near the interface provides a hybridization between majority- and minority-spin states. In a typical Fe/MgO/Fe MTJ, we solve the tunneling problem and show that the TMR ratio oscillates with a period of ∼3Å by varying the MgO thickness, consistent with previous and present experimental observations.

DOI: 10.1103/PhysRevB.111.L220406

The tunneling effect is one of the most fundamental phenomena in quantum mechanics originating from the wave nature of matter. In particular, quantum tunneling has played an important role for various topics in condensed matter physics. For example, in the case of *p-n* junctions, electrons tunnel through the depletion layer under large electric field, giving rise to negative differential resistance [1]. As another example, tunneling spectrum in a metal/insulator/superconductor junction provides a clear signature of a gap structure in the density of states of the superconductor, validating the Bardeen-Cooper-Schrieffer theory [2]. Moreover, the scanning tunneling microscope utilizes tunneling electrons for imaging surfaces in the atomic level [3].

The tunnel magnetoresistance (TMR) effect is another topic related to tunneling in the field of spintronics. This occurs in magnetic tunnel junctions (MTJs) consisting of an insulating barrier sandwiched between ferromagnetic electrodes [Fig. 1(a)]. The wave functions in different spin channels have different transmission probabilities because of imbalanced band structures, leading to finite magnetoresistance. One can estimate the magnitude of the magnetoresistance by defining the TMR ratio as a ratio of resistances between parallel and antiparallel magnetization states of the two ferromagnetic electrodes. In 2004, Parkin *et al.* [4] and Yuasa *et al.* [5] reported significantly high TMR ratios in Fe(Co)/MgO/Fe(Co)(001) MTJs, which provided a basis for further fundamental studies of the TMR effect and their device applications. However, there is a missing piece in the mechanism of such a giant TMR effect; the universal oscillation of the TMR ratio as a function of the insulating barrier thickness [5–8] has not been explained satisfactorily. In a report of the giant TMR effect in Fe/MgO/Fe(001) [5], Yuasa *et al.* observed an oscillation of the TMR ratio with a period of ∼3 Å by varying the MgO thickness, referred to as the TMR oscillation. Subsequent experiments [6] clarified that the TMR oscillation originates from resistance oscillations in both parallel and antiparallel magnetization states. Here, electron tunneling through MgO occurs between the same (different) spin states of the two electrodes in the parallel (antiparallel) magnetization state. Recent experiments for a series of MTJs with high crystallinity [9–11] found that the TMR oscillation with a period of ∼3 Å is universally observed and its amplitude is much larger than ever reported. Therefore, to elucidate the origin of the TMR oscillation will advance our understanding not only on the TMR effect but also on the quantum tunneling itself. This will also provide guiding principles for achieving even higher TMR ratios.

Conventionally, high TMR ratios in Fe/MgO/Fe(001) have been explained by the Δ_1 coherent tunneling mechanism; the half-metallic Δ_1 band structure of Fe [Figs. 1(b) and 1(c)] and the slowest decaying Δ_1 evanescent state of MgO enable a selective tunneling of the perfectly spin-polarized Δ_1 state, leading to a high TMR ratio [12,13]. However, the TMR oscillation cannot be explained by this mechanism [12–14]. Although additional effects, such as interference of evanescent states [12] and nonspecular tunneling [15], have been considered, these provide a resistance oscillation only in the antiparallel magnetization state, qualitatively in disagreement with the experimental results. Another study [16] proposed an

*Contact author: MASUDA.Keisuke@nims.go.jp

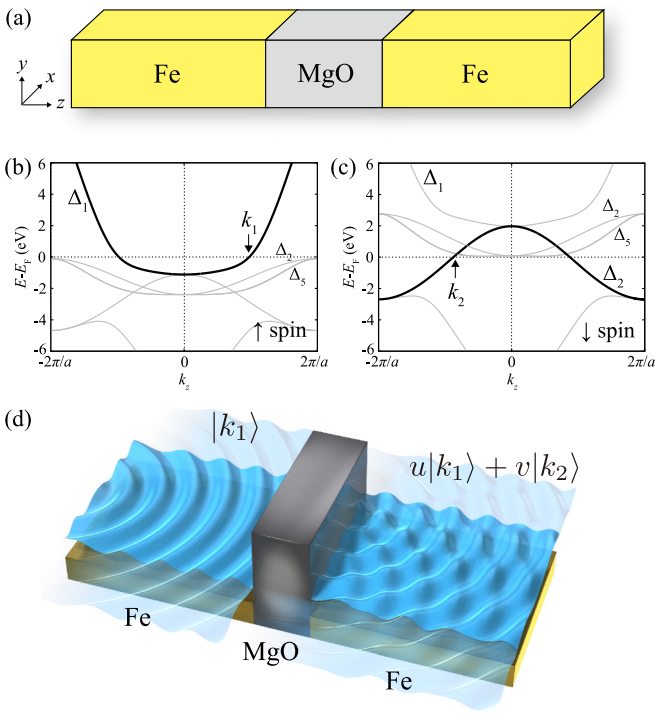

FIG. 1. (a) Schematic of the Fe/MgO/Fe MTJ. (b), (c) Majority (↑) -spin and minority (↓) -spin band structures of bcc Fe along the Δ line with $\mathbf{k}_\parallel = 0$. (d) Illustration of our idea including a superposition of wave functions with different Fermi momenta.

oscillation of the TMR ratio due to the quantization in the ferromagnetic layer, but this occurs when varying the thickness of the ferromagnetic layer, inconsistent with the experimental situation.

In this Letter, we show that the TMR oscillation can be explained by taking into account a superposition of wave functions with opposite spins and different Fermi momenta for the tunneling problem. It is known that spin-flip scattering occurs near interfaces of MTJs [17–19], indicating that spin is not a good quantum number in this system. This provides a hybridization between majority- and minority-spin states with different Fermi momenta [Figs. 1(b) and 1(c)], which justifies our assumption on the superposition of wave functions. Focusing on Fe/MgO/Fe(001), we solve tunneling problems assuming a superposition of majority-spin Δ_1 and minority-spin Δ_2 wave functions with different Fermi momenta as a transmitted wave function [see Fig. 1(d)]. We obtain transmittances in the parallel and antiparallel magnetization states, from which the TMR ratio is calculated. It is found that the transmittances and the TMR ratio have oscillatory behaviors with a period of ~ 3 Å as a function of the MgO thickness, in agreement with previous and present experimental observations. We also show that the calculated TMR ratio can reproduce our experimental results not only qualitatively but also quantitatively by tuning the parameters in our model. Although we focus on the TMR oscillation in this Letter, the superposition of wave functions with different Fermi momenta is a general concept and would be helpful to understand transport properties in other tunnel junctions with superconductors, semiconductors, etc.

To make the point of our approach clearer, we start by reviewing the conventional analytical treatment of the tunneling problem in an MTJ. Let us consider the situation that the wave function in the left electrode propagates to the right electrode passing through the insulating barrier, which is described by a coordinate system with the z axis along the stacking direction of the MTJ [Fig. 1(a)]. For simplicity, we focus on the wave functions with $\mathbf{k}_\parallel = (k_x, k_y) = (0, 0)$ providing the dominant contribution to tunneling transport. When the Fermi momentum is given by $k_z = k_\mathrm{L}$ (k_R) in the left (right) electrode, the wave function ψ_L (ψ_R) in the left (right) electrode and the wave function ψ_b in the insulating barrier are expressed as

$$\psi_\mathrm{L}(z) = e^{ik_\mathrm{L}z} + R\,e^{-ik_\mathrm{L}z}, \tag{1}$$

$$\psi_\mathrm{b}(z) = A\,e^{-\kappa z} + B\,e^{\kappa z}, \tag{2}$$

$$\psi_\mathrm{R}(z) = C\,e^{ik_\mathrm{R}z}, \tag{3}$$

where κ is the decaying wave number inside the insulating barrier. After determining R, A, B, and C from continuation conditions for the wave function and its derivative at $z = 0$ and d [20], we find the following expression for the transmittance:

$$T = \frac{16\,\tilde{k}_\mathrm{L}\kappa^2\tilde{k}_\mathrm{R}e^{2\kappa d}}{[\kappa(\tilde{k}_\mathrm{L}+\tilde{k}_\mathrm{R})(1+e^{2\kappa d})]^2 + [(\kappa^2-\tilde{k}_\mathrm{L}\tilde{k}_\mathrm{R})(1-e^{2\kappa d})]^2}, \tag{4}$$

where d is the thickness of the insulating barrier, $\tilde{k}_\mathrm{L} = (m_\mathrm{b}/m_\mathrm{L})\,k_\mathrm{L}$ and $\tilde{k}_\mathrm{R} = (m_\mathrm{b}/m_\mathrm{R})\,k_\mathrm{R}$. Here, $m_\mathrm{L(R)}$ and m_b are the effective masses in the left (right) electrode and the insulating barrier, respectively [32]. We can obtain the conductance G by substituting Eq. (4) into the Landauer formula $G = (e^2/h)\,T$. The Δ_1 coherent tunneling mechanism mentioned above can be confirmed by employing this tunneling theory in combination with the first-principles calculation [34–36].

However, this conventional tunneling theory cannot describe the oscillation of the TMR ratio in the Fe/MgO/Fe(001) MTJ. Actually, the transmittance in the parallel magnetization state is obtained by putting $k_\mathrm{L} = k_\mathrm{R} = k_1$ (or k_2) in Eq. (4), where k_1 and k_2 are the Fermi momenta of the majority-spin Δ_1 and the minority-spin Δ_2 bands of Fe, respectively [see Figs. 1(b) and 1(c)]. Note that the negative k_2 value with a positive group velocity is chosen for the minority-spin state, since we focus on right-moving states. The transmittance in the antiparallel magnetization state is similarly obtained by setting $k_\mathrm{L} = k_1$ (or k_2) and $k_\mathrm{R} = k_2$ (or k_1) in Eq. (4). As seen from Eq. (4), both the parallel and antiparallel transmittances decrease exponentially with increasing d in monotonic manner without any oscillations.

To explain the oscillation in the transmittance, we introduce a superposition of wave functions between the majority-spin Δ_1 and minority-spin Δ_2 states for the transmitted wave in the tunneling problem [37]. Details on the choice of these wave functions are discussed in the Supplemental Material [20]. Let us first calculate the parallel transmittance T_P. Based on the fact that the majority-spin Δ_1 state provides the dominant contribution to the TMR effect [12,13], T_P can be calculated as $T_\mathrm{P} = T_{\mathrm{P},\uparrow} + T_{\mathrm{P},\downarrow} \approx T_{\mathrm{P},\uparrow}$, where ↑ (↓) indicates that tunneling electrons are in the majority-spin

(minority-spin) state in the left electrode. For the calculation of $T_{\mathrm{P},\uparrow}$, we consider a tunneling from the majority-spin Δ_1 state in the left electrode to the superposition state in the right electrode with the dominant contribution from the majority-spin Δ_1 state, which is given by

$$\psi_{\mathrm{L}}(z) = e^{ik_{1z}} + R\, e^{-ik_{1z}}, \tag{5}$$

$$\psi_{\mathrm{b}}(z) = A\, e^{-\kappa z} + B\, e^{\kappa z}, \tag{6}$$

$$\psi_{\mathrm{R}}(z) = C\,(u\, e^{ik_{1z}} + v\, e^{ik_{2z}}). \tag{7}$$

Here, u and v are matrix elements of the unitary matrix that diagonalizes the 2×2 Hamiltonian, including the effect of the interfacial spin-flip scattering as off-diagonal elements. An explicit expression of the Hamiltonian and the derivation of the wave function in Eq. (7) are given in the Supplemental Material [20]. We impose $|u| \gg |v|$ because of the dominance of the majority-spin Δ_1 state in $T_{\mathrm{P},\uparrow}$. The matrix elements also satisfy the normalization condition $|u|^2 + |v|^2 = 1$. By using the continuity of the wave function and its derivative at $z = 0$ and d [38], we can derive the following expression for $T_{\mathrm{P},\uparrow}$:

$$T_{\mathrm{P},\uparrow} = \tilde{k}_{1\mathrm{L}}^{-1}[\tilde{u}^2\tilde{k}_{1\mathrm{R}} + \tilde{v}^2\tilde{k}_{2\mathrm{R}} + \tilde{u}\tilde{v}\,(\tilde{k}_{1\mathrm{R}} + \tilde{k}_{2\mathrm{R}})\cos((k_1 - k_2)d - \theta)]|C|^2, \tag{8}$$

$$\begin{aligned}\text{Denominator of } |C|^2 = {} & (e^{\kappa d} - e^{-\kappa d})^2\big\{\kappa^4[1 + 2\,\tilde{u}\tilde{v}\cos((k_1 - k_2)d - \theta)] \\ & - 2\,\kappa^2\tilde{k}_{1\mathrm{L}}[\tilde{u}^2\tilde{k}_{1\mathrm{R}} + \tilde{v}^2\tilde{k}_{2\mathrm{R}} + \tilde{u}\tilde{v}\,(\tilde{k}_{1\mathrm{R}} + \tilde{k}_{2\mathrm{R}})\cos((k_1 - k_2)d - \theta)] \\ & + \tilde{k}_{1\mathrm{L}}^2\big[\tilde{u}^2\tilde{k}_{1\mathrm{R}}^2 + \tilde{v}^2\tilde{k}_{2\mathrm{R}}^2 + 2\,\tilde{u}\tilde{v}\,\tilde{k}_{1\mathrm{R}}\tilde{k}_{2\mathrm{R}}\cos((k_1 - k_2)d - \theta)\big]\big\} \\ & + (e^{\kappa d} + e^{-\kappa d})^2\big\{\kappa^2\tilde{k}_{1\mathrm{L}}^2[1 + 2\,\tilde{u}\tilde{v}\cos((k_1 - k_2)d - \theta)] \\ & + 2\,\kappa^2\tilde{k}_{1\mathrm{L}}[\tilde{u}^2\tilde{k}_{1\mathrm{R}} + \tilde{v}^2\tilde{k}_{2\mathrm{R}} + \tilde{u}\tilde{v}\,(\tilde{k}_{1\mathrm{R}} + \tilde{k}_{2\mathrm{R}})\cos((k_1 - k_2)d - \theta)] \\ & + \kappa^2\big[\tilde{u}^2\tilde{k}_{1\mathrm{R}}^2 + \tilde{v}^2\tilde{k}_{2\mathrm{R}}^2 + 2\,\tilde{u}\tilde{v}\,\tilde{k}_{1\mathrm{R}}\tilde{k}_{2\mathrm{R}}\cos((k_1 - k_2)d - \theta)\big]\big\} \\ & + 2\,(e^{\kappa d} + e^{-\kappa d})(e^{\kappa d} - e^{-\kappa d})\,\tilde{u}\tilde{v}\,\big(\kappa^2 + \tilde{k}_{1\mathrm{L}}^2\big)\,\kappa\,(\tilde{k}_{1\mathrm{R}} - \tilde{k}_{2\mathrm{R}})\sin((k_1 - k_2)d - \theta)\end{aligned} \tag{9}$$

$$\text{Numerator of } |C|^2 = 16\,\tilde{k}_{1\mathrm{L}}^2\,\kappa^2, \tag{10}$$

where $\tilde{k}_{1\mathrm{L}} = (m_{\mathrm{b}}/m_{\mathrm{L}})\,k_1$, $\tilde{k}_{1\mathrm{R}} = (m_{\mathrm{b}}/m_{\mathrm{R}})\,k_1$, and $\tilde{k}_{2\mathrm{R}} = (m_{\mathrm{b}}/m_{\mathrm{R}})\,k_2$. We put $u = \tilde{u}$ and $v = \tilde{v}\,e^{i\theta}$ using positive real numbers $\tilde{u}$ and $\tilde{v}$. The relation $\tilde{u}^2 + \tilde{v}^2 = 1$ was used to simplify the expression. Equations (8) and (9) include several terms with $\cos((k_1 - k_2)\,d - \theta)$ or $\sin((k_1 - k_2)\,d - \theta)$, leading to an oscillation of the transmittance as a function of d. Physically speaking, this oscillation originates from the interference of the majority-spin Δ_1 and the minority-spin Δ_2 wave functions in the transmitted wave, which is seen from the analogy with the double-slit experiment in elementary quantum mechanics [20]. The antiparallel transmittance $T_{\mathrm{AP},\uparrow}$ is easily obtained by replacing $\tilde{u}$ with $\tilde{v}$ and $\tilde{v}$ with $-\tilde{u}$ in Eqs. (8)–(10) [39]. Since $\tilde{u} \gg \tilde{v}$, this replacement allows us to consider the transmittance for the electron tunneling from the majority-spin Δ_1 state in the left electrode to the superposition state in the right electrode with the dominant contribution from the minority-spin Δ_2 state, which corresponds to $T_{\mathrm{AP},\uparrow}$. Using $T_{\mathrm{AP},\uparrow}$, the total antiparallel transmittance can be calculated as $T_{\mathrm{AP}} = T_{\mathrm{AP},\uparrow} + T_{\mathrm{AP},\downarrow} \approx 2\,T_{\mathrm{AP},\uparrow}$. We simply set $\tilde{u} = 0.95$, $\theta = 0$, $m_{\mathrm{b}}/m_{\mathrm{L}} = 1.0$, and $m_{\mathrm{b}}/m_{\mathrm{R}} = 1.0$ (–1.0) for the numerical calculation of $T_{\mathrm{P},\uparrow}$ ($T_{\mathrm{AP},\uparrow}$); however, the period and overall shape of the oscillation in the transmittance do not change if we change $\tilde{u}$ within the range of $1 > \tilde{u} \gg \tilde{v}$. Note here that $m_{\mathrm{b}}/m_{\mathrm{L}}$ and $m_{\mathrm{b}}/m_{\mathrm{R}}$ need to have different signs in the antiparallel state, which is discussed in the Supplemental Material [20].

Figure 2 shows inverses of parallel and antiparallel transmittances, $T_{\mathrm{P},\uparrow}^{-1}$ and $T_{\mathrm{AP},\uparrow}^{-1}$, divided by the exponentially increasing factor $\exp(2\kappa d)$. Here, we set $\kappa = 0.2\pi/a_{\mathrm{MgO}}$ ($a_{\mathrm{MgO}} = 4.217$ Å: lattice constant of MgO), which is the decaying wave number for the Δ_1 complex band of MgO calculated by the PWCOND code [40]. We also used $k_1 = 1.0\pi/a_{\mathrm{Fe}}$ and $k_2 = -0.9\pi/a_{\mathrm{Fe}}$ ($a_{\mathrm{Fe}} = 2.866$ Å: lattice constant of bcc Fe) obtained by calculating the band structure of bcc Fe [Figs. 1(b) and 1(c)] with the aid of QUANTUM ESPRESSO [41]. In both $T_{\mathrm{P},\uparrow}^{-1}$ and $T_{\mathrm{AP},\uparrow}^{-1}$, we can see a clear oscillation with a period of $2\pi/(k_1 - k_2)$. From the values of k_1 and k_2 mentioned above, the period is estimated to be $\sim$3 Å. These are consistent with the experimental fact that resistances in both the parallel and antiparallel magnetization states have oscillatory barrier thickness dependencies with

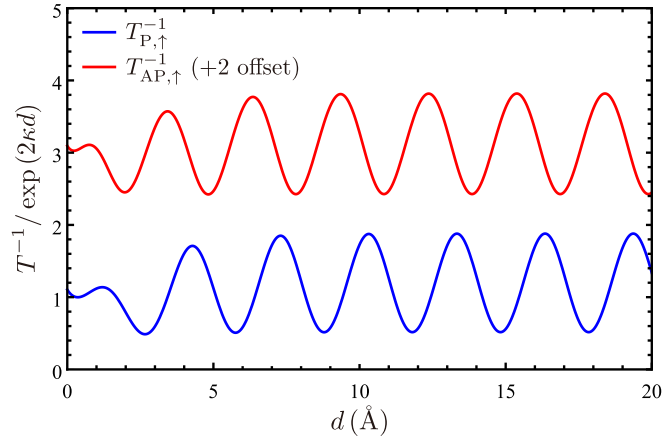

FIG. 2. Barrier thickness d dependencies of inverses of parallel and antiparallel transmittances, $T_{\mathrm{P},\uparrow}^{-1}$ and $T_{\mathrm{AP},\uparrow}^{-1}$, divided by $\exp(2\kappa d)$.

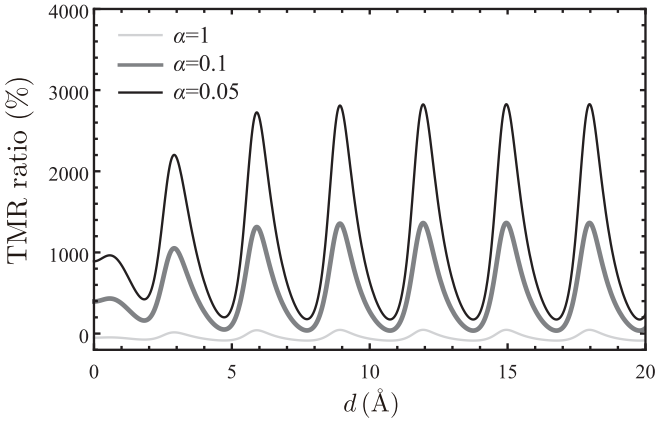

FIG. 3. TMR ratios as a function of the barrier thickness d for different values of α. This was obtained by Eq. (11).

periods of ∼3 Å [6,10,11]. Finally, we would like to point out that either shape or phase in the oscillation needs to have a difference between $T_{\mathrm{P},\uparrow}^{-1}$ and $T_{\mathrm{AP},\uparrow}^{-1}$ for the occurrence of the TMR oscillation shown in Fig. 3 [42].

By using $T_{\mathrm{P},\uparrow}$ and $T_{\mathrm{AP},\uparrow}$, we calculated the TMR ratio given by

$$(T_{\mathrm{P}} - \alpha\, T_{\mathrm{AP}})/\alpha\, T_{\mathrm{AP}} \approx (T_{\mathrm{P},\uparrow} - 2\,\alpha\, T_{\mathrm{AP},\uparrow})/2\,\alpha\, T_{\mathrm{AP},\uparrow}. \quad (11)$$

Here, we introduced an electronic-structure parameter α, by which T_{AP} is scaled relative to T_{P} reflecting electronic structures of Fe and MgO. The case with $\alpha = 1$ corresponds to the usual definition of the TMR ratio. However, as shown in Fig. 3, the TMR ratio takes negative values for $\alpha = 1$, inconsistent with positive high TMR ratios observed in experiments. This is because the present analysis employs only the values of the Fermi momenta and the decaying wave number and does not consider detailed electronic structures of Fe and MgO. If these electronic structures are taken into account by using the first-principles calculation [12,13], values of T_{AP} are around one order of magnitude smaller than those of T_{P}. Thus, we set $\alpha = 0.1$ for a better comparison with experimental values of the TMR ratio obtained at room temperature in Fig. 4(b) [43]. Figure 3 shows barrier thickness d dependencies of the TMR ratio for different values of α. For all values of α, the TMR ratio shows an oscillation with a period of $2\pi/(k_1 - k_2) \sim 3$ Å, similarly to $T_{\mathrm{P},\uparrow}^{-1}$ and $T_{\mathrm{AP},\uparrow}^{-1}$.

Let us directly compare our calculation results with an experimentally observed TMR oscillation. To this aim, we fabricated an MTJ structure and measured magnetotransport properties. The experimental method is explained in the Supplemental Material [20]. Figure 4(a) shows barrier thickness d dependencies of the resistance-area product (RA) in the parallel and antiparallel magnetization states, where RA is a product of the resistance and the cross-sectional area of the MTJ. We show values of the RA divided by $\exp(a \cdot d + b)$, where a and b were determined to be 5.48 (5.73) nm^{-1} and −2.36 (−1.35) in the parallel (antiparallel) magnetization state, respectively, from the fits using the exponential function. As seen in Fig. 4(a), the RA has an oscillatory d dependence with a period of 3.1 Å in both the parallel and antiparallel magnetization states [44]. We also find that both the shape and phase of the RA oscillation are slightly different between

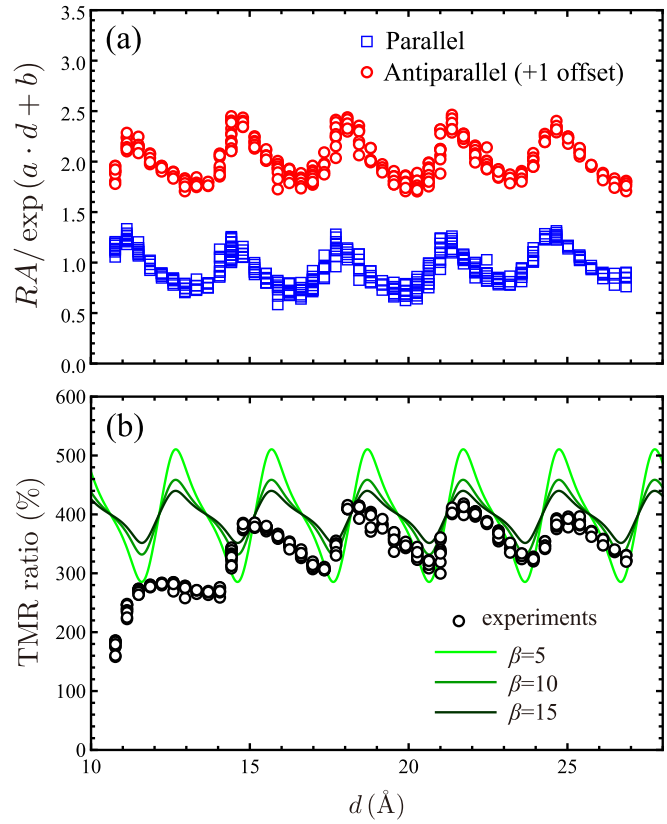

FIG. 4. Experimental results of (a) RA values and (b) TMR ratios in Fe/Mg_4AlO_x/Fe(001) at room temperature. Panel (b) also shows theoretical values of TMR ratios for different values of β calculated by Eq. (12) with $\alpha = 0.1$ [47].

the parallel and antiparallel magnetization states [45], leading to the TMR oscillation in Fig. 4(b). For a direct comparison between theoretical and experimental results, we recalculated the TMR ratio using

$$[(T_{\mathrm{P}} + \beta\, e^{-2\kappa d}) - \alpha\,(T_{\mathrm{AP}} + \beta\, e^{-2\kappa d})]/\alpha\,(T_{\mathrm{AP}} + \beta\, e^{-2\kappa d}), \quad (12)$$

where α is fixed to 0.1. Note here that another parameter β is introduced for transmittances at $\mathbf{k}_{\parallel} \neq 0$ [46]. In the derivation of Eqs. (8)–(10), we considered only the electronic states at $\mathbf{k}_{\parallel} = 0$ because of its dominant contribution to the TMR effect. However, in actual experiments, electronic states at $\mathbf{k}_{\parallel} \neq 0$ can also contribute to the transmission, which is expressed by the β-related terms in Eq. (12). Since transmittances at different $\mathbf{k}_{\parallel}$ should have different periods of oscillations, these oscillations are mixed and cancel each other. Thus, we treated the β-related terms as simple exponential functions. In Fig. 4(b), calculated TMR ratios for different values of β are compared with experimental results. We find that a saw-tooth-like shape of the TMR oscillation is quite similar between theoretical and experimental results [48]. In addition, the TMR ratios calculated for $\beta = 15$ are found to quantitatively agree with experimental values. Therefore, we conclude that the TMR ratio calculated by Eq. (12) can reproduce the experimental results not only qualitatively but also

quantitatively. To further validate our theory, we have conducted additional experiments and discussed the relation with previous experiments using Heusler alloys, which are explained in the Supplemental Material [20].

In summary, we proposed a theory for explaining the universal oscillation of the TMR ratio called the TMR oscillation. Based on the fact that spin-flip scattering occurs near interfaces of MTJs, we took into account the superposition of the majority-spin Δ_1 and minority-spin Δ_2 wave functions with different Fermi momenta for the tunneling problem in Fe/MgO/Fe(001). We analytically calculated transmittances in the parallel and antiparallel magnetization states, from which the TMR ratio was obtained. It was found that the transmittances and the TMR ratio have oscillatory barrier thickness dependencies with a period of ∼3 Å, consistent with the experimental observations. According to our theory, the period of the TMR oscillation is determined by the difference of the Fermi momenta between the majority- and minority-spin states in the ferromagnetic electrode. Therefore, the period of ∼3 Å is specific to bcc Fe used as electrodes. If MTJs with other ferromagnetic electrodes are successfully made, TMR oscillations with periods different from 3 Å would be observed. We expect future experimental studies using a wider range of materials will provide further information for the TMR oscillation.

The authors are grateful to S. Yuasa and H. Imamura for fruitful discussions. The authors also thank S. Kasai for magnetotransport measurements and H. Ikeda for her technical support on device microfabrication. This work was supported by Grants-in-Aid for Scientific Research (Grants No. 22H04966, No. 23K03933, and No. 24H00408) and MEXT Program: Data Creation and Utilization-Type Material Research and Development Project (Grant No. JPMXP1122715503). MANA is supported by the World Premier International Research Center Initiative (WPI) of MEXT, Japan. The band structure calculation was performed on the Numerical Materials Simulator at NIMS.

[1] L. Esaki, New phenomenon in narrow germanium *p–n* junctions, Phys. Rev. **109**, 603 (1958).

[2] I. Giaever, Energy gap in superconductors measured by electron tunneling, Phys. Rev. Lett. **5**, 147 (1960).

[3] G. Binnig and H. Rohrer, Scanning tunneling microscopy—from birth to adolescence, Rev. Mod. Phys. **59**, 615 (1987).

[4] S. S. P. Parkin, C. Kaiser, A. Panchula, P. M. Rice, B. Hughes, M. Samant, and S.-H. Yang, Giant tunnelling magnetoresistance at room temperature with MgO (100) tunnel barriers, Nat. Mater. **3**, 862 (2004).

[5] S. Yuasa, T. Nagahama, A. Fukushima, Y. Suzuki, and K. Ando, Giant room-temperature magnetoresistance in single-crystal Fe/MgO/Fe magnetic tunnel junctions, Nat. Mater. **3**, 868 (2004).

[6] R. Matsumoto, A. Fukushima, T. Nagahama, Y. Suzuki, K. Ando, and S. Yuasa, Oscillation of giant tunneling magnetoresistance with respect to tunneling barrier thickness in fully epitaxial Fe/MgO/Fe magnetic tunnel junctions, Appl. Phys. Lett. **90**, 252506 (2007).

[7] T. Ishikawa, S. Hakamata, K.-i. Matsuda, T. Uemura, and M. Yamamoto, Fabrication of fully epitaxial Co_2MnSi/MgO/Co_2MnSi magnetic tunnel junctions, J. Appl. Phys. **103**, 07A919 (2008).

[8] T. Marukame, T. Ishikawa, T. Taira, K. I. Matsuda, T. Uemura, and M. Yamamoto, Giant oscillations in spin-dependent tunneling resistances as a function of barrier thickness in fully epitaxial magnetic tunnel junctions with a MgO barrier, Phys. Rev. B **81**, 134432 (2010).

[9] T. Scheike, Q. Xiang, Z. Wen, H. Sukegawa, T. Ohkubo, K. Hono, and S. Mitani, Exceeding 400% tunnel magnetoresistance at room temperature in epitaxial Fe/MgO/Fe(001) spin-valve-type magnetic tunnel junctions, Appl. Phys. Lett. **118**, 042411 (2021).

[10] T. Scheike, Z. Wen, H. Sukegawa, and S. Mitani, Enhanced tunnel magnetoresistance in Fe/Mg_4Al-O_x/Fe(001) magnetic tunnel junctions, Appl. Phys. Lett. **120**, 032404 (2022).

[11] T. Scheike, Z. Wen, H. Sukegawa, and S. Mitani, 631% room temperature tunnel magnetoresistance with large oscillation effect in CoFe/MgO/CoFe(001) junctions, Appl. Phys. Lett. **122**, 112404 (2023).

[12] W. H. Butler, X.-G. Zhang, T. C. Schulthess, and J. M. MacLaren, Spin-dependent tunneling conductance of Fe|MgO|Fe sandwiches, Phys. Rev. B **63**, 054416 (2001).

[13] J. Mathon and A. Umerski, Theory of tunneling magnetoresistance of an epitaxial Fe/MgO/Fe(001) junction, Phys. Rev. B **63**, 220403(R) (2001).

[14] C. Heiliger, P. Zahn, B. Y. Yavorsky, and I. Mertig, Thickness dependence of the tunneling current in the coherent limit of transport, Phys. Rev. B **77**, 224407 (2008).

[15] X.-G. Zhang, Y. Wang, and X. F. Han, Theory of nonspecular tunneling through magnetic tunnel junctions, Phys. Rev. B **77**, 144431 (2008).

[16] G. Autès, J. Mathon, and A. Umerski, Oscillatory behavior of tunnel magnetoresistance in a magnetic tunnel junction with varying magnetic layer thickness, Phys. Rev. B **84**, 134404 (2011).

[17] P. Mavropoulos, M. Lezaic, and S. Blügel, Half-metallic ferromagnets for magnetic tunnel junctions by *ab initio* calculations, Phys. Rev. B **72**, 174428 (2005).

[18] Y. Miura, K. Abe, and M. Shirai, Effects of interfacial noncollinear magnetic structures on spin-dependent conductance in Co_2MnSi/MgO/Co_2MnSi magnetic tunnel junctions: A first-principles study, Phys. Rev. B **83**, 214411 (2011).

[19] K. Masuda, T. Tadano, and Y. Miura, Crucial role of interfacial *s-d* exchange interaction in the temperature dependence of tunnel magnetoresistance, Phys. Rev. B **104**, L180403 (2021).

[20] See Supplemental Material at http://link.aps.org/supplemental/10.1103/PhysRevB.111.L220406 for the basis of our theory, continuation conditions, treatment of effective masses, choice of wave functions, model for the interfacial spin-flip scattering,

analogy with the double-slit experiment, the experimental method, further experimental results, and the relation with experiments using Heusler alloys, which includes Refs. [7,8,21–31].

[21] J. H. Davies, *The Physics of Low-Dimensional Semiconductors* (Cambridge University Press, Cambridge, UK, 1998).

[22] D. J. BenDaniel and C. B. Duke, Space-charge effects on electron tunneling, Phys. Rev. **152**, 683 (1966).

[23] J. R. Schrieffer and P. A. Wolff, Relation between the Anderson and Kondo Hamiltonians, Phys. Rev. **149**, 491 (1966).

[24] J. Korringa, On the calculation of the energy of a Bloch wave in a metal, Physica **13**, 392 (1947).

[25] W. Kohn and N. Rostoker, Solution of the Schrödinger equation in periodic lattices with an application to metallic lithium, Phys. Rev. **94**, 1111 (1954).

[26] AkaiKKR (Machikaneyama), http://kkr.issp.u-tokyo.ac.jp.

[27] J. P. Perdew, K. Burke, and M. Ernzerhof, Generalized gradient approximation made simple, Phys. Rev. Lett. **77**, 3865 (1996).

[28] P. Soven, Coherent-potential model of substitutional disordered alloys, Phys. Rev. **156**, 809 (1967).

[29] S. Ishida, S. Fujii, S. Kashiwagi, and S. Asano, Search for half-metallic compounds in Co_2MnZ (Z=IIIb, IVb, Vb Element), J. Phys. Soc. Jpn. **64**, 2152 (1995).

[30] I. Galanakis, P. H. Dederichs, and N. Papanikolaou, Slater-Pauling behavior and origin of the half-metallicity of the full-Heusler alloys, Phys. Rev. B **66**, 174429 (2002).

[31] O. Gaier, J. Hamrle, S. J. Hermsdoerfer, H. Schultheiß, B. Hillebrands, Y. Sakuraba, M. Oogane, and Y. Ando, Influence of the $L2_1$ ordering degree on the magnetic properties of Co_2MnSi Heusler films, J. Appl. Phys. **103**, 103910 (2008).

[32] If we set $m_L = m_b = m_R$, Eq. (4) coincides with Eq. (3) in Ref. [33], where different effective masses are not considered.

[33] J. M. MacLaren, X.-G. Zhang, and W. H. Butler, Validity of the Julliere model of spin-dependent tunneling, Phys. Rev. B **56**, 11827 (1997).

[34] Y. Miura, S. Muramoto, K. Abe, and M. Shirai, First-principles study of tunneling magnetoresistance in $Fe/MgAl_2O_4/Fe(001)$ magnetic tunnel junctions, Phys. Rev. B **86**, 024426 (2012).

[35] K. Masuda and Y. Miura, First-principles study on magnetic tunneling junctions with semiconducting $CuInSe_2$ and $CuGaSe_2$ barriers, Jpn. J. Appl. Phys. **56**, 020306 (2017).

[36] K. Masuda and Y. Miura, Bias voltage effects on tunneling magnetoresistance in $Fe/MgAl_2O_4/Fe(001)$ junctions: Comparative study with Fe/MgO/Fe(001) junctions, Phys. Rev. B **96**, 054428 (2017).

[37] We also considered a similar superposition of wave functions in the incident and reflection waves. This additional analysis clarified that these do not affect the oscillatory behavior of the transmittance given by the superposition in the transmitted wave. Thus, we omit these effects for simplicity.

[38] We used the same continuation conditions as mentioned in the Supplemental Material.

[39] This is because $T_{AP,\uparrow}$ can be calculated by using $\psi_R(z) = C(-v^* e^{ik_1 z} + u e^{ik_2 z})$ instead of Eq. (7).

[40] A. Smogunov, A. D. Corso, and E. Tosatti, Ballistic conductance of magnetic Co and Ni nanowires with ultrasoft pseudopotentials, Phys. Rev. B **70**, 045417 (2004).

[41] P. Giannozzi, S. Baroni, N. Bonini, M. Calandra, R. Car, C. Cavazzoni, D. Ceresoli, G. L. Chiarotti, M. Cococcioni, I. Dabo, A. D. Corso, S. de Gironcoli, S. Fabris, G. Fratesi, R. Gebauer, U. Gerstmann, C. Gougoussis, A. Kokalj, M. Lazzeri, L. Martin-Samos *et al.*, Quantum ESPRESSO: A modular and open-source software project for quantum simulations of materials, J. Phys.: Condens. Matter **21**, 395502 (2009).

[42] In our results, differences in both the shape and phase between the $T_{P,\uparrow}^{-1}$ and $T_{AP,\uparrow}^{-1}$ oscillations provide the TMR oscillation. Although the oscillation shapes of $T_{P,\uparrow}^{-1}$ and $T_{AP,\uparrow}^{-1}$ look quite similar, these have a slight difference owing to the difference in the effective mass and the replacement of the coefficients (u and v) in the expression of the transmittance.

[43] TMR ratios at low temperature are more than twice as high as those at room temperature and can be reproduced by using a smaller value of α.

[44] The amplitude of the *RA* oscillation hardly changes as the barrier thickness d increases, consistent with the results in Fig. 2. In our theory, the amplitude of the transmittance oscillation is determined by the values of u and v in Eq. (7). Since u and v are assumed to be constant, the amplitude of the oscillation hardly changes with increasing d. This assumption is reasonable, since the interfacial exchange interaction determining u and v is independent on d.

[45] Note that the phase difference in *RA* is smaller than that in the inverse of the transmittance in Fig. 2; however, this does not mean that our theory is inconsistent with experimental observations [5,6,8–11]. It is experimentally known that the phase difference highly depends on the quality of the sample and is not a universal feature for the TMR oscillation.

[46] We introduced nonoscillatory terms $\beta e^{-2\kappa d}$ decreasing exponentially as the barrier thickness increases.

[47] For a better comparison with experimental results, we applied a shift in d by 0.8 Å for Eq. (12).

[48] Experimentally, the shape of the TMR oscillation is different for different samples. Actually, Mg_4AlO_x-based MTJs have sawtooth-like shapes [10] similarly to our present results, while MgO-based MTJs have sinelike shapes [9,11]. These different shapes can be reproduced by tuning the parameters in our model.